GEOPHYSICAL RESEARCH LETTERS, VOL. 20, NO. 20, PAGES 2267-2270, OCTOBER 22, 1993

THREE VIEWS OF TWO GIANT STREAMS: ALIGNED OBSERVATIONS AT 1 AU, 4.6 AU, AND 5.9 AU

George Siscoe and Devrie Intriligator

Carmel Research Center

Abstract. A close radial alignment of the IMP and Pioneers 10 and 11 spacecraft in 1974 allows a nearly unambiguous, empirical study of the radial evolution of the interaction regions of two contrasting weak and strong, giant streams. The study confirms the main aspects of the standard model of corotating interaction regions: an expanding and strengthening pair of forward-reverse shocks sandwich a stream interface. It adds the following concepts: stream group speed--the speed at the stream interface tends to remain constant with distance; corotating stream complexes--interaction regions can include features like noncompressive density enhancements and streamer belts; secondary interfaces--a possible precursor to the reverse shock; and emerging stream interfaces--one emerged between 1 AU and 4.6 AU. The study uses the conservation specific entropy to correlate features between spacecraft.

Introduction

In 1974 two giant solar wind streams recurred on ten successive solar rotations, presenting ideal subject matter for research on corotating streams. Also at this time Pioneer 11, at 4.6 AU, and Pioneer 10, at 5.9 AU, monitored the streams while residing within a ten degree, sun-centered wedge. And for one solar rotation--Bartels Rotation Number 1929--Earth and its IMP satellites shared the wedge. This conjunction provides soundings of virtually the same pieces of the two streams at widely separated distances. These soundings give nearly unambiguous, empirically derived pictures of two instances of radial stream evolution. Here we describe their basic features.

Much is known observationally and theoretically about the radial evolution of corotating streams. Thus not unexpectedly, the pictures found here confirm the standard model of the leading edges of such streams, which are also known as corotating interaction regions (CIRs) [e.g., Smith and Wolfe, 1976; Gosling et al., 1978; Gazis, 1987]. One stream possesses a well developed stream interface (SI) separating an upstream, low-entropy regime from a downstream, high-entropy regime [Burlaga, 1974]. Data on the other stream evidently catch a stream interface in the act of forming: no trace of an SI appears at 1 AU, but a nascent SI is present at 4.6 AU. For both streams, forward and reverse shocks develop between 2 AU and 4.6 AU [cf., Hundhausen and Gosling, 1976; Gosling, et al., 1976].

This study augments the standard CIR model by adding noncompressive density enhancements [Gosling et al., 1977] and the heliospheric current sheet [Smith et al., 1978] with its streamer belt [Borrini et al., 1981; Gosling et al., 1981]. It also adds at 1 AU a previously unreported intermediate-entropy plateau between the stream interface and the following, high-entropy fast stream. We refer to the augmented corotating interaction region--containing one or more incidental features such as streamer belt, heliospheric current sheet, and noncompressive density enhancements--as a corotating stream complex (CSC).

Paper number 93GL02488
0094-8534/93/93GL-02488$03.00

A word on the distinction between CIRs and CSCs is in order: whereas CIRs have the same set of defining features--a stream interface sandwiched between forward and reverse shocks--CSCs are CIRs with features that are not creations of the interaction; that is features that are incidental to it. Thus whereas one CIR differs from another only in degree of heliographic tilt and speed of evolution, one CSC differs from another also in its inventory of structural elements. Another way to state the distinction is that whereas CIRs can be isomorphically transformed into an archetypical CIR, in general, CSCs cannot be isomorphically transformed into an archetypal CSC, though there might be a finite set of archetypes. This is not to say that one cannot construct a model that represents a general CSC; indeed, these case studies lead to such a model.

The Streams of Solar Rotation 1929 at 1 AU

To set baseline conditions against which to measure radial stream evolution, we describe the situation at 1 AU at the IMP satellites. Both streams had recurred already ten times before their appearance in rotation 1929, which extends from August 18 to September 14, 1974 [King, 1977]. By then they had revealed their distinctive and, as it turns out, complementary properties. Each filled approximately half of the 27 day synodic rotation period. Stream 1 emanated from an equator-crossing, peninsula-like extension of the northern polar coronal hole. Stream 2 emanated from an equator-grazing extension of the southern polar coronal hole [Hundhausen, 1977 and 1993, private communication].

Figure 1 shows four-day intervals of solar wind and interplanetary magnetic field (IMF) data per-

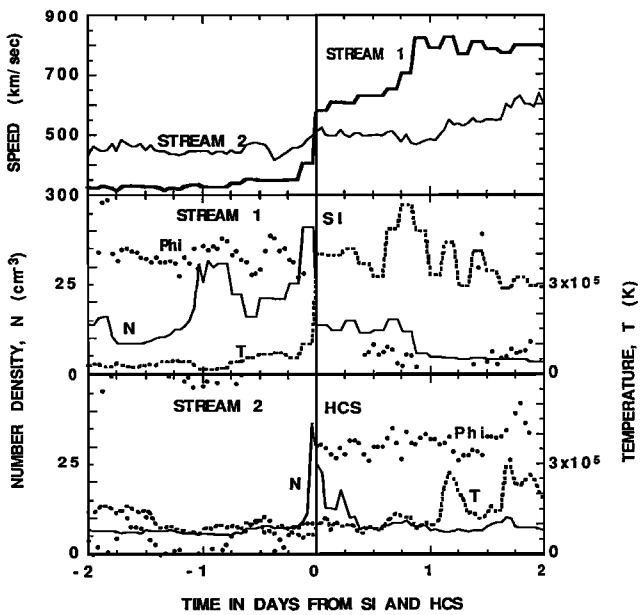

Fig. 1 One-hour averages at 1 AU of the solar wind speed, number density (N), temperature (T), and IMF ecliptic longitude angle (Phi). The data cover two stretches of four days in 1974 centered on day 231.37 for stream 1 and day 241.50 for stream 2.

taining to the leading edges of the streams. For stream 1, the interval is centered on the stream interface; for stream 2, which has no stream interface at 1 AU, it is centered on the heliospheric current sheet. Stream 1 is the faster and more abrupt of the two streams: its speed more than doubles in the first tenth of its ca. ten day duration, peaking at more than 800 km/sec. It has a distinct, narrow stream interface which coincides with the steepest rise in speed. The stream interface is marked by a sharp decrease in density that coincides with an equally sudden increase in temperature; or in terms of a single parameter, it is marked by an abrupt increase in the specific entropy. The stream interface requires less than an hour to pass the spacecraft. The heliospheric current sheet associated with this stream passes the spacecraft within three hours prior to the passage of the stream interface. A data gap precludes closer timing. On earlier recurrences, the heliospheric current sheet precedes the arrival of the stream interface by intervals of 2 and 15 hours. Here and on all but one prior recurrence, the streamer belt, which ensheathes the heliospheric current sheet, forms part of the density feature whose decrease defines the stream interface.

In contrast with the fast, 100% speed increase for stream 1, stream 2 requires half of its duration to reach a peak speed of under 700 km/sec, an increase of only 50%. Its associated streamer belt is narrow and prominent. The absence of an accompanying temperature increase means that there is no stream interface at 1 AU. The stream's previous recurrence, however, displayed a well defined stream interface. The narrow and pronounced high density streamer belt and the constant temperature create a correspondingly narrow and pronounced dip in the specific entropy as discussed below.

Radial Stream Evolution

Figure 2 shows the solar wind speed history for rotation 1929 as recorded by the three spacecraft. The data intervals are aligned on the passage of the stream interface of stream 1, which is defined to within one or two hours at each station. At the Pioneers it coincides also to within one or two hours with the passage of the heliospheric current sheet.

Stream 1 exhibits the characteristic features of the standard stream evolution model [Hundhausen and Gosling, 1976]: By 4.6 AU forward and reverse shocks have formed and have already created an intershock region which requires three days to pass the spacecraft. By 5.9 AU, passage of the intershock region requires more than four days. Between the shocks the speed is nearly constant at

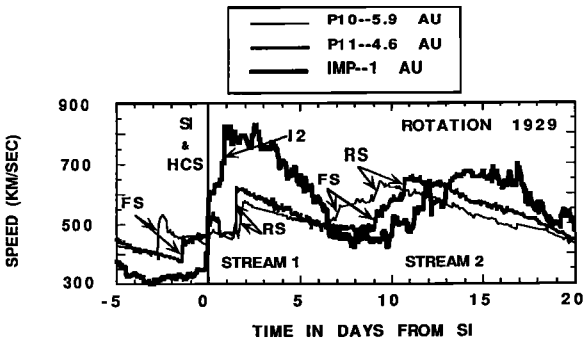

Fig. 2 Solar wind speed at 1 AU, 4.6 AU, and 5.9 AU for Bartels Rotation 1929. These 25-day intervals in 1974 are aligned on days 231.37 for IMP, 218.85 for Pioneer 11, and 224.05 for Pioneer 10. Marked features are the following: FS, forward shock, RS, reverse shock, SI, stream interface; HSC heliospheric current sheet; I2, secondary interface.

both spacecraft and between both spacecraft. This common speed, about 450 km/sec, is seen nearly to coincide with the speed at the stream interface at 1 AU. It is as if the stream advances from 1 AU to 5.9 AU at the speed of the stream interface, which remains constant with distance. Evidently the forward shock accelerates the slow, preceding wind and the reverse shock decelerates the fast, following wind to maintain a nearly constant speed at the stream interface. We refer to this common speed as the stream's group speed. (The speed pulses lasting less than one day following the stream interface at Pioneer 11 and the forward shock at Pioneer 10 are anomalous. They do not appear on earlier recurrences of this stream.)

An important point of clarification is in order. It appears that the stream interface is advecting with the plasma rather than propagating through it. This follows since the stream interface retains its position relative to the heliospheric current sheet, which is also, presumably, nonpropagating. When the passage of both features can be timed, the heliospheric current sheet always precedes the stream interface. For stream 1, the two features often virtually coincide from 1 to 5.9 AU. The usual interpretation of this is that both features are nonpropagating discontinuities in the plasma. There is another argument supporting advection over propagation. Thought of as a MHD discontinuity, the stream interface does not satisfy the criteria for propagation: it is not a shock because the density and temperature increment in opposite directions; and it is not a rotational discontinuity because the density and temperature change across it.

In Figure 2, the stream interface is not a shock so its shock-like speed jump at 1 AU is not a precursor of the forward shocks at 4.6 and 5.9 AU. Similarly, the speed jump at 1 AU occurring about one day after the passage of the stream interface is not a reverse shock, which it resembles, since, as Figure 3 shows, the specific entropy increased when the feature passed. This is the wrong sense of change for a reverse shock. Unlike the stream interface, however, which maintains its character with distance, this feature might evolve into a reverse shock farther out. To distinguish the two speed-jump features at 1 AU, we label the trailing one the secondary interface. Then from the low-entropy streamer belt to the high-entropy fast stream, the entropy increases in two steps marked by the two interfaces. The intermediate-entropy plateau between the interfaces is present on most recurrences of stream 1. As Figure 1 shows, the intermediate-entropy plateau is associated with a shoulder-like extension into the domain of the fast stream of the density feature that defines the stream interface. There is a similar extension of the streamer belt density for stream 2. A cursory look at other corotating streams finds enough instances of asymmetrical density features of the type described to suggest a common underlying structural or dynamical cause. (A statistical analysis is needed to quantify this observation.) Perhaps these density extensions are a variant of the snowplow model [Neugebauer and Snyder, 1966] that adds a "brick wall" in the form of the narrow, high-density streamer belt. In this variant, the fast stream shoves overtaken, intermediate-entropy plasma against a relatively immobile, high-inertia obstacle. The secondary interface would then be the leading edge of the backwash of an expanding "pile" of plasma. As such, it could evolve into a reverse shock. Indeed, Zhao [1992] identifies one instance of a secondary interface at a reverse shock.

Though stream 2 is weaker than stream 1, distinct forward-reverse shock pairs are evident at both Pioneers, but the intershock speed is not as constant. Though the shocks are reducing the contrast between the extremes of low and high speeds, the average speed from 1 to 5.9 AU is nearly constant at about 550 km/sec. Thus stream

2 has a group speed which is about 100 km/sec faster than the group speed of stream 1. The difference in group speeds results in stream 2 gaining on stream 1. At 5.9 AU stream 2 is about four days nearer to stream 1 than at 1 AU. This appears to be an example of evolution towards a merged interaction region [Burlaga, 1984].

The structure of the stream interaction regions and their contrasts with the pure stream regions is most concisely shown through plots of specific entropy, of the ions, which is proportional to $\ln(T_i/n^{\gamma-1})$, where T_i is ion temperature, n is number density, γ is the polytropic index. The advantage of such plots is that specific entropy tends to be a constant of motion. Thus it acts as a flow marker. Also, significant changes in it signal dissipation processes, like shocks. Figure 3 shows specific entropy plots for the same intervals and the same alignment as Figure 2. For comparison the values are overlain in the top panel, and for legibility they are separated by one decade in the bottom panel. The curves track each other remarkably well on the trailing portions of both streams. To obtain the close coincidence of values in these portions, we used $\gamma = 3/2$ instead of the 5/3 that corresponds to the ideal, adiabatic case. This lower value for γ agrees with the methodical determination of Totten [1993] for the free-streaming solar wind.

With one exception, the major departures from coincidence of the curves occur in the interaction regions between the shocks. The exception happens during the first three and a half days of the plot, when the values at 1 AU are generally less than farther out. At this time there are two exceptionally low "valleys"--one wide and one narrow--which correspond to noncompressive density enhancements. NCDEs are by definition low-entropy features [Gosling et al., 1977]. The narrow NCDE is not a streamer belt, for it contains no heliospheric current sheet, and as Figure 1 shows, it is well separated from the actual streamer belt. This NCDE does not recur, but the preceding, wide NCDE (which lies outside the border of Figure 1) appears on several preceding rotations. The forward shock, which formed between 1 and 4.6 AU, increased the entropy within the narrow NCDE and most of the wide NCDE. The remaining unshocked part of the wide NCDE appears as the narrow, low-entropy feature through which the shock at 4.6 AU is propagating. By 4.6 AU the relatively fast group speed of stream 1 shifted these features closer to the stream interface. The point of the example is that NCDEs that happen to lie upstream from SIs at 1 AU turn into shocked, advecting entropy-contrast layers that structure the intershock zone of a mature interaction region.

Despite the layering of stream 1's interaction region, the entropy generally drops from the forward shock to the stream interface, which reflects the fact that the strength of the shock increases with heliocentric distance at least to 5.9 AU. At the forward shocks of both Pioneers, the entropy argument jumps by more than an order of magnitude. Between the Pioneer 11 forward shock and the stream interface, the Pioneer curves essentially coincide, reconfirming the γ calibration and the constancy property of the specific entropy. The comparison also suggests that the forward shock forms fairly close to the stream interface, for starting essentially there, the Pioneer values are higher than the IMP values. At the interface itself, across which the entropy increases rapidly at all three spacecraft, the three values essentially coincide, indicating a relative lack of dissipation at this central marker. But almost immediately thereafter, the entropies at the Pioneers, while tracking each other, again reach values higher than at IMP. This suggests that the reverse shock also forms fairly close to the stream interface, though the brief interval of high entropy preceding the reverse shock might otherwise indicate a remoter origin. It is simpler to accommodate the observations by supposing the secondary stream interface, as it evolves from 1 to 4.6 AU, first being shifted towards the stream interface by differential advection until it aligns with the Pioneer curves, then becoming the reverse shock which creates an expanding plateau of elevated entropy that reaches the point where the Pioneers find it. In this scenario the terminal, brief interval of high entropy would require a sudden increase in shock strength, for which no explanation is obvious in these data. Even with this terminal entropy pulse, the change in the entropy argument across the reverse shock is less than an order of magnitude. Thus the reverse shock is considerably weaker than the forward shock at the same distance.

The shocks for stream 2 are weak. Although

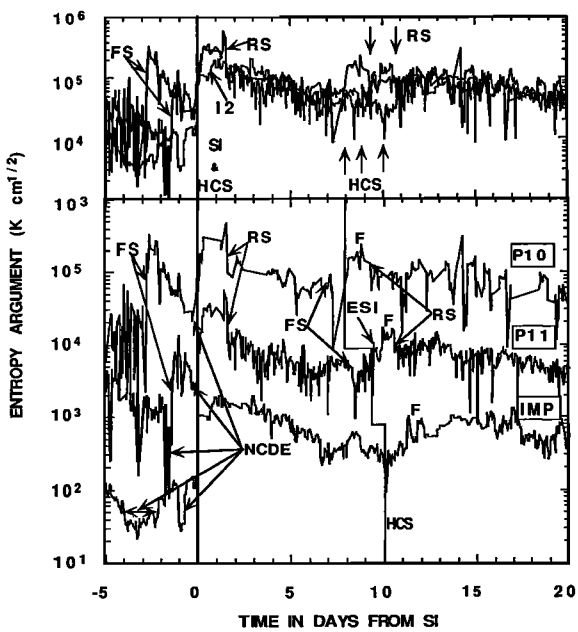

Fig. 3 Specific entropy argument ($T/n^{\gamma-1}$ with $\gamma = 1.5$) at 1 AU, 4.6 AU, and 5.9 AU for the same intervals as in Fig. 2. The entropies are overlain in the top panel and separated by one decade in the bottom panel. Additional marked features are the following: ESI, emerged stream interface; NCDE, noncompressive density enhancements; F, an entropy marker.

they are marked by abrupt increases in density, temperature, and field strength, the entropy increases are small or undetectable. The FS and RS arrows for Pioneer 11 point to where the shocks are identified in the other data sets, but are undetectable as entropy changes. By Pioneer 10 the shocks have strengthened to detectability as entropy changes. The advance of stream 2 on stream 1 is seen in the progression from spacecraft to spacecraft of the shocks, the heliospheric current sheet, and a fortuitous entropy marker labeled F. (The trailing edge of this marker resembles, but is not, the reverse shock.) The heliospheric current sheet does not coincide with the lowest entropy dip at Pioneer 11, as it does at IMP. (The HCS line has been displaced slightly to the left to expose the entropy dips marking the streamer belt.) The lowest entropy dip at Pioneer 11 is an anomalous feature, which occurs immediately following the forward shock. The dip comprises several consecutive measurements of abnormally low temperatures, and so is probably real. Its origin is unknown. The low entropy dip associated with the streamer belt is very distinct and coincides with the heliospheric current sheet. At Pioneer 10 a data gap hides the heliospheric current sheet and the streamer belt. The HCS line is drawn near the middle of the gap. The extraordinary entropy dip following the forward shock at Pioneer 10 comprises a single density outlier, and might not be real.

In stream 2 there is the appearance at Pioneer 11 of a stream interface, which has apparently emerged between 1 AU and 4.6 AU. At Pioneer 10 it is hidden by the data gap. The entropy argument nearly doubles from the downstream to the upstream side of the streamer belt at Pioneer 11, whereas at IMP it returns to the downstream value. The emerged stream interface arises mainly through an increase in temperature; the density returns nearly to its prestreamer-belt value. This increase cannot be attributed to the action of the reverse shock between 1 AU and 4.6 AU, for the reverse shock is unable to increase the entropy even at 4.6 AU. A dissipation process stronger than the reverse shock, perhaps associated with velocity shear, is operating beyond 1 AU. If this is the generic process that creates stream interfaces, it operates inside of 1 AU for strong streams and outside of 1 AU for weak streams. Then the origin of stream interfaces becomes a synthesis of the in-transit compression model of Hundhausen and Burlaga [1975] and the coronal, velocity shear idea advocated by Gosling et al. [1978].

Conclusions

The radial evolution of a corotating interaction region can be richly varied because of the inclusion within it of indigenous or exogenous incidental features and because of the variable emergence of standard CIR features. At least from 1 AU to 5.9 AU, CIRs tend to move with a constant speed, intermediate between the lowest and highest values for the stream. Specific entropy is a highly useful quantity for interspacecraft comparisons.

Acknowledgments. We are indebted to the Pioneer Project Office for the success of Pioneers 10 and 11. IMP data were obtained from the NSSDC. Pioneer 10 and 11 plasma and magnetic field parameters were obtained from A. Barnes and E.J. Smith, respectively. This work was supported by NASA Ames Research Center under contract NAS2-13692 and by Carmel Research Center.

References

Borrini, G., J.T. Gosling, S.J. Bame, W.C. Feldman, and J.M. Wilcox, Solar wind helium and hydrogen structure near the heliospheric current sheet: A signal of coronal streamers at 1 AU, J. Geophys. Res., 86, 4565-4573, 1981.

Burlaga, L.F., Interplanetary stream interfaces, J. Geophys. Res., 79, 3717-3725, 1974.

Burlaga, L.F., MHD processes in the outer heliosphere, Space Sci. Rev., 39, 255, 1984.

Burlaga, L.F., Multifractal structure of the magnetic field and plasma in recurrent streams at 1 AU, J. Geophys. Res., 97, 4283-4293, 1992.

Gazis, P.R., Solar wind stream structure at large heliospheric distances, J. Geophys. Res., 92, 2231-2242, 1987.

Gosling, J.T., E. Hildner, R.M. MacQueen, R.H. Munro, A.I. Poland, and C.L. Ross, Mass ejections from the sun: A view from Skylab, J. Geophys. Res., 79, 4581-4587, 1974.

Gosling, J.T., A.J. Hundhausen, and S.J. Bame, Solar wind stream evolution at large heliocentric distances: Experimental demonstration and the test of a model, J. Geophys. Res., 81, 2111-2122, 1976.

Gosling, J.T., E. Hildner, J.R. Asbridge, S.J. Bame, and W.C. Feldman, Noncompressive density enhancements in the solar wind, J. Geophys. Res., 82, 5005-5010, 1977.

Gosling, J.T., J.R. Asbridge, S.J. Bame, and W.C. Feldman, Solar wind stream interfaces, J. Geophys. Res., 83, 1401-1412, 1978.

Gosling, J.T., G. Borrini, J.R. Asbridge, S.J. Bame, W.C. Feldman, and R.T. Hansen, Coronal streamers in the solar wind at 1 AU, J. Geophys. Res., 86, 5438-5448, 1981.

Hundhausen, A.J., and L.F. Burlaga, A model of the origin of solar wind stream interfaces, J. Geophys. Res., 80, 1845-1848, 1975.

Hundhausen, A.J., and J.T. Gosling, Solar wind structure at large heliocentric distances: An interpretation of Pioneer 10 observations, J. Geophys. Res., 81, 1436-1440, 1976.

Hundhausen, A.J., An interplanetary view of coronal holes, in Coronal Holes and High Speed Wind Streams, edited by J.B. Zirker, Colorado Associated University Press, pp. 226, 1977.

King, J. II., Interplanetary Medium Book, NSSDC/WDC-A R&S77-04, 1977.

Neugebauer, M., and C.W. Snyder, Mariner-2 measurements of the solar wind, in The Solar Wind, edited by R.J. Mackin, Jr., and M. Neugebauer, Pergamon Press, pp. 3-24, 1966.

Smith, E.J., and J.H. Wolfe, Observations of interaction regions and corotating shocks between one and five AU: Pioneers 10 and 11, Geophys. Res. Lett., 3, 137, 1976.

Smith, E.J., B.T. Tsurutani, and R.L. Rosenberg, Observations of the interplanetary sector structure up to heliographic latitudes of 16°: Pioneer 11, J. Geophys. Res., 83, 717-724, 1978.

Totten, T.L., Determination of the polytropic index of the free streaming solar wind, MS Thesis, Rice University, 1993.

Zhao, X., Interaction of fast steady flow with slow transient flow: A new cause of shock pair and interplanetary Bz event, J. Geophys. Res., 97, 15,051-15,055, 1992.

George Siscoe and Devrie Intriligator, Carmel Research Center, P.O. Box 1732, Santa Monica, CA 90406.

(Received: August 6, 1993;
accepted: August 20, 1993.)